EUROPEAN ORGANIZATION FOR NUCLEAR RESEARCH (CERN)

arXiv:1305.5059v1 [hep-ex] 22 May 2013

Search for the rare decay $D^0 \to \mu^+\mu^-$

The LHCb collaboration[†]

Abstract

A search for the rare decay $D^0 \to \mu^+\mu^-$ is performed using a data sample, corresponding to an integrated luminosity of 0.9 fb^{-1}, of pp collisions collected at a centre-of-mass energy of 7 TeV by the LHCb experiment. The observed number of events is consistent with the background expectations and corresponds to an upper limit of $\mathcal{B}(D^0 \to \mu^+\mu^-) < 6.2\,(7.6) \times 10^{-9}$ at 90% (95%) confidence level. This result represents an improvement of more than a factor twenty with respect to previous measurements.

[†]Authors are listed on the following pages.

LHCb collaboration

R. Aaij[40], C. Abellan Beteta[35,n], B. Adeva[36], M. Adinolfi[45], C. Adrover[6], A. Affolder[51],
Z. Ajaltouni[5], J. Albrecht[9], F. Alessio[37], M. Alexander[50], S. Ali[40], G. Alkhazov[29],
P. Alvarez Cartelle[36], A.A. Alves Jr[24,37], S. Amato[2], S. Amerio[21], Y. Amhis[7], L. Anderlini[17,f],
J. Anderson[39], R. Andreassen[56], R.B. Appleby[53], O. Aquines Gutierrez[10], F. Archilli[18],
A. Artamonov[34], M. Artuso[57], E. Aslanides[6], G. Auriemma[24,m], S. Bachmann[11], J.J. Back[47],
C. Baesso[58], V. Balagura[30], W. Baldini[16], R.J. Barlow[53], C. Barschel[37], S. Barsuk[7],
W. Barter[46], Th. Bauer[40], A. Bay[38], J. Beddow[50], F. Bedeschi[22], I. Bediaga[1], S. Belogurov[30],
K. Belous[34], I. Belyaev[30], E. Ben-Haim[8], G. Bencivenni[18], S. Benson[49], J. Benton[45],
A. Berezhnoy[31], R. Bernet[39], M.-O. Bettler[46], M. van Beuzekom[40], A. Bien[11], S. Bifani[44],
T. Bird[53], A. Bizzeti[17,h], P.M. Bjørnstad[53], T. Blake[37], F. Blanc[38], J. Blouw[11], S. Blusk[57],
V. Bocci[24], A. Bondar[33], N. Bondar[29], W. Bonivento[15,*], S. Borghi[53], A. Borgia[57],
T.J.V. Bowcock[51], E. Bowen[39], C. Bozzi[16], T. Brambach[9], J. van den Brand[41], J. Bressieux[38],
D. Brett[53], M. Britsch[10], T. Britton[57], N.H. Brook[45], H. Brown[51], I. Burducea[28],
A. Bursche[39], G. Busetto[21,q], J. Buytaert[37], S. Cadeddu[15], O. Callot[7], M. Calvi[20,j],
M. Calvo Gomez[35,n], A. Camboni[35], P. Campana[18,37], D. Campora Perez[37], A. Carbone[14,c],
G. Carboni[23,k], R. Cardinale[19,i], A. Cardini[15], H. Carranza-Mejia[49], L. Carson[52],
K. Carvalho Akiba[2], G. Casse[51], L. Castillo Garcia[37], M. Cattaneo[37], Ch. Cauet[9],
M. Charles[54], Ph. Charpentier[37], P. Chen[3,38], N. Chiapolini[39], M. Chrzaszcz[25], K. Ciba[37],
X. Cid Vidal[37], G. Ciezarek[52], P.E.L. Clarke[49], M. Clemencic[37], H.V. Cliff[46], J. Closier[37],
C. Coca[28], V. Coco[40], J. Cogan[6], E. Cogneras[5], P. Collins[37], A. Comerma-Montells[35],
A. Contu[15,37], A. Cook[45], M. Coombes[45], S. Coquereau[8], G. Corti[37], B. Couturier[37],
G.A. Cowan[49], D.C. Craik[47], S. Cunliffe[52], R. Currie[49], C. D'Ambrosio[37], P. David[8],
P.N.Y. David[40], A. Davis[56], I. De Bonis[4], K. De Bruyn[40], S. De Capua[53], M. De Cian[39],
J.M. De Miranda[1], L. De Paula[2], W. De Silva[56], P. De Simone[18], D. Decamp[4],
M. Deckenhoff[9], L. Del Buono[8], N. Déléage[4], D. Derkach[14], O. Deschamps[5], F. Dettori[41],
A. Di Canto[11], F. Di Ruscio[23,k], H. Dijkstra[37], M. Dogaru[28], S. Donleavy[51], F. Dordei[11],
A. Dosil Suárez[36], D. Dossett[47], A. Dovbnya[42], F. Dupertuis[38], R. Dzhelyadin[34], A. Dziurda[25],
A. Dzyuba[29], S. Easo[48,37], U. Egede[52], V. Egorychev[30], S. Eidelman[33], D. van Eijk[40],
S. Eisenhardt[49], U. Eitschberger[9], R. Ekelhof[9], L. Eklund[50,37], I. El Rifai[5], Ch. Elsasser[39],
D. Elsby[44], A. Falabella[14,e], C. Färber[11], G. Fardell[49], C. Farinelli[40], S. Farry[12], V. Fave[38],
D. Ferguson[49], V. Fernandez Albor[36], F. Ferreira Rodrigues[1], M. Ferro-Luzzi[37], S. Filippov[32],
M. Fiore[16], C. Fitzpatrick[37], M. Fontana[10], F. Fontanelli[19,i], R. Forty[37], O. Francisco[2],
M. Frank[37], C. Frei[37], M. Frosini[17,f], S. Furcas[20], E. Furfaro[23,k], A. Gallas Torreira[36],
D. Galli[14,c], M. Gandelman[2], P. Gandini[57], Y. Gao[3], J. Garofoli[57], P. Garosi[53],
J. Garra Tico[46], L. Garrido[35], C. Gaspar[37], R. Gauld[54], E. Gersabeck[11], M. Gersabeck[53],
T. Gershon[47,37], Ph. Ghez[4], V. Gibson[46], V.V. Gligorov[37], C. Göbel[58], D. Golubkov[30],
A. Golutvin[52,30,37], A. Gomes[2], H. Gordon[54], M. Grabalosa Gándara[5], R. Graciani Diaz[35],
L.A. Granado Cardoso[37], E. Graugés[35], G. Graziani[17], A. Grecu[28], E. Greening[54],
S. Gregson[46], P. Griffith[44], O. Grünberg[59], B. Gui[57], E. Gushchin[32], Yu. Guz[34,37], T. Gys[37],
C. Hadjivasiliou[57], G. Haefeli[38], C. Haen[37], S.C. Haines[46], S. Hall[52], T. Hampson[45],
S. Hansmann-Menzemer[11], N. Harnew[54], S.T. Harnew[45], J. Harrison[53], T. Hartmann[59],
J. He[37], V. Heijne[40], K. Hennessy[51], P. Henrard[5], J.A. Hernando Morata[36],
E. van Herwijnen[37], A. Hicheur[1], E. Hicks[51], D. Hill[54], M. Hoballah[5], M. Holtrop[40],
C. Hombach[53], P. Hopchev[4], W. Hulsbergen[40], P. Hunt[54], T. Huse[51], N. Hussain[54],

D. Hutchcroft[51], D. Hynds[50], V. Iakovenko[43], M. Idzik[26], P. Ilten[12], R. Jacobsson[37],
A. Jaeger[11], E. Jans[40], P. Jaton[38], F. Jing[3], M. John[54], D. Johnson[54], C.R. Jones[46],
C. Joram[37], B. Jost[37], M. Kaballo[9], S. Kandybei[42], M. Karacson[37], T.M. Karbach[37],
I.R. Kenyon[44], U. Kerzel[37], T. Ketel[41], A. Keune[38], B. Khanji[20], O. Kochebina[7],
I. Komarov[38], R.F. Koopman[41], P. Koppenburg[40], M. Korolev[31], A. Kozlinskiy[40],
L. Kravchuk[32], K. Kreplin[11], M. Kreps[47], G. Krocker[11], P. Krokovny[33], F. Kruse[9],
M. Kucharczyk[20,25,j], V. Kudryavtsev[33], T. Kvaratskheliya[30,37], V.N. La Thi[38], D. Lacarrere[37],
G. Lafferty[53], A. Lai[15], D. Lambert[49], R.W. Lambert[41], E. Lanciotti[37], G. Lanfranchi[18],
C. Langenbruch[37], T. Latham[47], C. Lazzeroni[44], R. Le Gac[6], J. van Leerdam[40], J.-P. Lees[4],
R. Lefèvre[5], A. Leflat[31], J. Lefrançois[7], S. Leo[22], O. Leroy[6], T. Lesiak[25], B. Leverington[11],
Y. Li[3], L. Li Gioi[5], M. Liles[51], R. Lindner[37], C. Linn[11], B. Liu[3], G. Liu[37], S. Lohn[37],
I. Longstaff[50], J.H. Lopes[2], E. Lopez Asamar[35], N. Lopez-March[38], H. Lu[3], D. Lucchesi[21,q],
J. Luisier[38], H. Luo[49], F. Machefert[7], I.V. Machikhiliyan[4,30], F. Maciuc[28], O. Maev[29,37],
S. Malde[54], G. Manca[15,d], G. Mancinelli[6], U. Marconi[14], R. Märki[38], J. Marks[11],
G. Martellotti[24], A. Martens[8], L. Martin[54], A. Martín Sánchez[7], M. Martinelli[40],
D. Martinez Santos[41], D. Martins Tostes[2], A. Massafferri[1], R. Matev[37], Z. Mathe[37],
C. Matteuzzi[20], E. Maurice[6], A. Mazurov[16,32,37,e], J. McCarthy[44], A. McNab[53], R. McNulty[12],
B. Meadows[56,54], F. Meier[9], M. Meissner[11], M. Merk[40], D.A. Milanes[8], M.-N. Minard[4],
J. Molina Rodriguez[58], S. Monteil[5], D. Moran[53], P. Morawski[25], M.J. Morello[22,s],
R. Mountain[57], I. Mous[40], F. Muheim[49], K. Müller[39], R. Muresan[28], B. Muryn[26], B. Muster[38],
P. Naik[45], T. Nakada[38], R. Nandakumar[48], I. Nasteva[1], M. Needham[49], N. Neufeld[37],
A.D. Nguyen[38], T.D. Nguyen[38], C. Nguyen-Mau[38,p], M. Nicol[7], V. Niess[5], R. Niet[9],
N. Nikitin[31], T. Nikodem[11], A. Nomerotski[54], A. Novoselov[34], A. Oblakowska-Mucha[26],
V. Obraztsov[34], S. Oggero[40], S. Ogilvy[50], O. Okhrimenko[43], R. Oldeman[15,d], M. Orlandea[28],
J.M. Otalora Goicochea[2], P. Owen[52], A. Oyanguren[35,o], B.K. Pal[57], A. Palano[13,b],
M. Palutan[18], J. Panman[37], A. Papanestis[48], M. Pappagallo[50], C. Parkes[53], C.J. Parkinson[52],
G. Passaleva[17], G.D. Patel[51], M. Patel[52], G.N. Patrick[48], C. Patrignani[19,i],
C. Pavel-Nicorescu[28], A. Pazos Alvarez[36], A. Pellegrino[40], G. Penso[24,l], M. Pepe Altarelli[37],
S. Perazzini[14,c], D.L. Perego[20,j], E. Perez Trigo[36], A. Pérez-Calero Yzquierdo[35], P. Perret[5],
M. Perrin-Terrin[6], G. Pessina[20], K. Petridis[52], A. Petrolini[19,i], A. Phan[57],
E. Picatoste Olloqui[35], B. Pietrzyk[4], T. Pilař[47], D. Pinci[24], S. Playfer[49], M. Plo Casasus[36],
F. Polci[8], G. Polok[25], A. Poluektov[47,33], E. Polycarpo[2], A. Popov[34], D. Popov[10],
B. Popovici[28], C. Potterat[35], A. Powell[54], J. Prisciandaro[38], A. Pritchard[51], C. Prouve[7],
V. Pugatch[43], A. Puig Navarro[38], G. Punzi[22,r], W. Qian[4], J.H. Rademacker[45],
B. Rakotomiaramanana[38], M.S. Rangel[2], I. Raniuk[42], N. Rauschmayr[37], G. Raven[41],
S. Redford[54], M.M. Reid[47], A.C. dos Reis[1], S. Ricciardi[48], A. Richards[52], K. Rinnert[51],
V. Rives Molina[35], D.A. Roa Romero[5], P. Robbe[7], E. Rodrigues[53], P. Rodriguez Perez[36],
S. Roiser[37], V. Romanovsky[34], A. Romero Vidal[36], J. Rouvinet[38], T. Ruf[37], F. Ruffini[22],
H. Ruiz[35], P. Ruiz Valls[35,o], G. Sabatino[24,k], J.J. Saborido Silva[36], N. Sagidova[29], P. Sail[50],
B. Saitta[15,d], V. Salustino Guimaraes[2], C. Salzmann[39], B. Sanmartin Sedes[36], M. Sannino[19,i],
R. Santacesaria[24], C. Santamarina Rios[36], E. Santovetti[23,k], M. Sapunov[6], A. Sarti[18,l],
C. Satriano[24,m], A. Satta[23], M. Savrie[16,e], D. Savrina[30,31], P. Schaack[52], M. Schiller[41],
H. Schindler[37], M. Schlupp[9], M. Schmelling[10], B. Schmidt[37], O. Schneider[38], A. Schopper[37],
M.-H. Schune[7], R. Schwemmer[37], B. Sciascia[18], A. Sciubba[24], M. Seco[36], A. Semennikov[30],
K. Senderowska[26], I. Sepp[52], N. Serra[39], J. Serrano[6], P. Seyfert[11], M. Shapkin[34],
I. Shapoval[16,42], P. Shatalov[30], Y. Shcheglov[29], T. Shears[51,37], L. Shekhtman[33],

iv

O. Shevchenko[42], V. Shevchenko[30], A. Shires[52], R. Silva Coutinho[47], T. Skwarnicki[57],
N.A. Smith[51], E. Smith[54,48], M. Smith[53], M.D. Sokoloff[56], F.J.P. Soler[50], F. Soomro[18],
D. Souza[45], B. Souza De Paula[2], B. Spaan[9], A. Sparkes[49], P. Spradlin[50], F. Stagni[37],
S. Stahl[11], O. Steinkamp[39], S. Stoica[28], S. Stone[57], B. Storaci[39], M. Straticiuc[28],
U. Straumann[39], V.K. Subbiah[37], L. Sun[56], S. Swientek[9], V. Syropoulos[41], M. Szczekowski[27],
P. Szczypka[38,37], T. Szumlak[26], S. T'Jampens[4], M. Teklishyn[7], E. Teodorescu[28], F. Teubert[37],
C. Thomas[54], E. Thomas[37], J. van Tilburg[11], V. Tisserand[4], M. Tobin[38], S. Tolk[41],
D. Tonelli[37], S. Topp-Joergensen[54], N. Torr[54], E. Tournefier[4,52], S. Tourneur[38], M.T. Tran[38],
M. Tresch[39], A. Tsaregorodtsev[6], P. Tsopelas[40], N. Tuning[40], M. Ubeda Garcia[37], A. Ukleja[27],
D. Urner[53], U. Uwer[11], V. Vagnoni[14], G. Valenti[14], R. Vazquez Gomez[35],
P. Vazquez Regueiro[36], S. Vecchi[16], J.J. Velthuis[45], M. Veltri[17,g], G. Veneziano[38],
M. Vesterinen[37], B. Viaud[7], D. Vieira[2], X. Vilasis-Cardona[35,n], A. Vollhardt[39],
D. Volyanskyy[10], D. Voong[45], A. Vorobyev[29], V. Vorobyev[33], C. Voß[59], H. Voss[10], R. Waldi[59],
R. Wallace[12], S. Wandernoth[11], J. Wang[57], D.R. Ward[46], N.K. Watson[44], A.D. Webber[53],
D. Websdale[52], M. Whitehead[47], J. Wicht[37], J. Wiechczynski[25], D. Wiedner[11], L. Wiggers[40],
G. Wilkinson[54], M.P. Williams[47,48], M. Williams[55], F.F. Wilson[48], J. Wishahi[9], M. Witek[25],
S.A. Wotton[46], S. Wright[46], S. Wu[3], K. Wyllie[37], Y. Xie[49,37], F. Xing[54], Z. Xing[57], Z. Yang[3],
R. Young[49], X. Yuan[3], O. Yushchenko[34], M. Zangoli[14], M. Zavertyaev[10,a], F. Zhang[3],
L. Zhang[57], W.C. Zhang[12], Y. Zhang[3], A. Zhelezov[11], A. Zhokhov[30], L. Zhong[3], A. Zvyagin[37].

[1]*Centro Brasileiro de Pesquisas Físicas (CBPF), Rio de Janeiro, Brazil*
[2]*Universidade Federal do Rio de Janeiro (UFRJ), Rio de Janeiro, Brazil*
[3]*Center for High Energy Physics, Tsinghua University, Beijing, China*
[4]*LAPP, Université de Savoie, CNRS/IN2P3, Annecy-Le-Vieux, France*
[5]*Clermont Université, Université Blaise Pascal, CNRS/IN2P3, LPC, Clermont-Ferrand, France*
[6]*CPPM, Aix-Marseille Université, CNRS/IN2P3, Marseille, France*
[7]*LAL, Université Paris-Sud, CNRS/IN2P3, Orsay, France*
[8]*LPNHE, Université Pierre et Marie Curie, Université Paris Diderot, CNRS/IN2P3, Paris, France*
[9]*Fakultät Physik, Technische Universität Dortmund, Dortmund, Germany*
[10]*Max-Planck-Institut für Kernphysik (MPIK), Heidelberg, Germany*
[11]*Physikalisches Institut, Ruprecht-Karls-Universität Heidelberg, Heidelberg, Germany*
[12]*School of Physics, University College Dublin, Dublin, Ireland*
[13]*Sezione INFN di Bari, Bari, Italy*
[14]*Sezione INFN di Bologna, Bologna, Italy*
[15]*Sezione INFN di Cagliari, Cagliari, Italy*
[16]*Sezione INFN di Ferrara, Ferrara, Italy*
[17]*Sezione INFN di Firenze, Firenze, Italy*
[18]*Laboratori Nazionali dell'INFN di Frascati, Frascati, Italy*
[19]*Sezione INFN di Genova, Genova, Italy*
[20]*Sezione INFN di Milano Bicocca, Milano, Italy*
[21]*Sezione INFN di Padova, Padova, Italy*
[22]*Sezione INFN di Pisa, Pisa, Italy*
[23]*Sezione INFN di Roma Tor Vergata, Roma, Italy*
[24]*Sezione INFN di Roma La Sapienza, Roma, Italy*
[25]*Henryk Niewodniczanski Institute of Nuclear Physics Polish Academy of Sciences, Kraków, Poland*
[26]*AGH - University of Science and Technology, Faculty of Physics and Applied Computer Science, Kraków, Poland*
[27]*National Center for Nuclear Research (NCBJ), Warsaw, Poland*
[28]*Horia Hulubei National Institute of Physics and Nuclear Engineering, Bucharest-Magurele, Romania*
[29]*Petersburg Nuclear Physics Institute (PNPI), Gatchina, Russia*

[30] *Institute of Theoretical and Experimental Physics (ITEP), Moscow, Russia*

[31] *Institute of Nuclear Physics, Moscow State University (SINP MSU), Moscow, Russia*

[32] *Institute for Nuclear Research of the Russian Academy of Sciences (INR RAN), Moscow, Russia*

[33] *Budker Institute of Nuclear Physics (SB RAS) and Novosibirsk State University, Novosibirsk, Russia*

[34] *Institute for High Energy Physics (IHEP), Protvino, Russia*

[35] *Universitat de Barcelona, Barcelona, Spain*

[36] *Universidad de Santiago de Compostela, Santiago de Compostela, Spain*

[37] *European Organization for Nuclear Research (CERN), Geneva, Switzerland*

[38] *Ecole Polytechnique Fédérale de Lausanne (EPFL), Lausanne, Switzerland*

[39] *Physik-Institut, Universität Zürich, Zürich, Switzerland*

[40] *Nikhef National Institute for Subatomic Physics, Amsterdam, The Netherlands*

[41] *Nikhef National Institute for Subatomic Physics and VU University Amsterdam, Amsterdam, The Netherlands*

[42] *NSC Kharkiv Institute of Physics and Technology (NSC KIPT), Kharkiv, Ukraine*

[43] *Institute for Nuclear Research of the National Academy of Sciences (KINR), Kyiv, Ukraine*

[44] *University of Birmingham, Birmingham, United Kingdom*

[45] *H.H. Wills Physics Laboratory, University of Bristol, Bristol, United Kingdom*

[46] *Cavendish Laboratory, University of Cambridge, Cambridge, United Kingdom*

[47] *Department of Physics, University of Warwick, Coventry, United Kingdom*

[48] *STFC Rutherford Appleton Laboratory, Didcot, United Kingdom*

[49] *School of Physics and Astronomy, University of Edinburgh, Edinburgh, United Kingdom*

[50] *School of Physics and Astronomy, University of Glasgow, Glasgow, United Kingdom*

[51] *Oliver Lodge Laboratory, University of Liverpool, Liverpool, United Kingdom*

[52] *Imperial College London, London, United Kingdom*

[53] *School of Physics and Astronomy, University of Manchester, Manchester, United Kingdom*

[54] *Department of Physics, University of Oxford, Oxford, United Kingdom*

[55] *Massachusetts Institute of Technology, Cambridge, MA, United States*

[56] *University of Cincinnati, Cincinnati, OH, United States*

[57] *Syracuse University, Syracuse, NY, United States*

[58] *Pontifícia Universidade Católica do Rio de Janeiro (PUC-Rio), Rio de Janeiro, Brazil, associated to [2]*

[59] *Institut für Physik, Universität Rostock, Rostock, Germany, associated to [11]*

∗ *Corresponding author.*

E-mail address: Walter.Bonivento@cern.ch

[a] *P.N. Lebedev Physical Institute, Russian Academy of Science (LPI RAS), Moscow, Russia*

[b] *Università di Bari, Bari, Italy*

[c] *Università di Bologna, Bologna, Italy*

[d] *Università di Cagliari, Cagliari, Italy*

[e] *Università di Ferrara, Ferrara, Italy*

[f] *Università di Firenze, Firenze, Italy*

[g] *Università di Urbino, Urbino, Italy*

[h] *Università di Modena e Reggio Emilia, Modena, Italy*

[i] *Università di Genova, Genova, Italy*

[j] *Università di Milano Bicocca, Milano, Italy*

[k] *Università di Roma Tor Vergata, Roma, Italy*

[l] *Università di Roma La Sapienza, Roma, Italy*

[m] *Università della Basilicata, Potenza, Italy*

[n] *LIFAELS, La Salle, Universitat Ramon Llull, Barcelona, Spain*

[o] *IFIC, Universitat de Valencia-CSIC, Valencia, Spain*

[p] *Hanoi University of Science, Hanoi, Viet Nam*

[q] *Università di Padova, Padova, Italy*

[r] *Università di Pisa, Pisa, Italy*

[s] *Scuola Normale Superiore, Pisa, Italy*

1 Introduction

Flavour-changing neutral current (FCNC) processes are highly suppressed in the Standard Model (SM) since they are only allowed at loop level and are affected by Glashow-Iliopoulos-Maiani (GIM) suppression [1]. They have been extensively studied in processes that involve K and B mesons. In D meson decays, FCNC processes are even more suppressed by the GIM mechanism, due to the absence of a high-mass down-type quark. The $D^0 \to \mu^+\mu^-$ decay is very rare in the SM because of additional helicity suppression. The short distance perturbative contribution to the branching fraction ($\mathcal{B}$) is of the order of 10^{-18} while the long distance non-perturbative contribution, dominated by the two-photon intermediate state, is about $2.7 \times 10^{-5} \times \mathcal{B}(D^0 \to \gamma\gamma)$ [2]. The current upper limit on $\mathcal{B}(D^0 \to \gamma\gamma)$ of 2.2×10^{-6} at 90% confidence level (CL) [3] translates into an upper bound for the SM prediction for $\mathcal{B}(D^0 \to \mu^+\mu^-)$ of about 6×10^{-11}. Given the current upper limit on $\mathcal{B}(D^0 \to \mu^+\mu^-)$ of 1.4×10^{-7} at 90% CL [4], there is therefore more than three orders of magnitude in $\mathcal{B}(D^0 \to \mu^+\mu^-)$ to be explored before reaching the sensitivity of the theoretical prediction.

Different types of beyond the Standard Model (BSM) physics could contribute to $D^0 \to \mu^+\mu^-$ decays and some could give enhancements with respect to the short distance SM prediction of several orders of magnitude. These include R-parity violating models [2, 5] and models with Randall-Sundrum warped extra dimensions [6], with predictions for $\mathcal{B}(D^0 \to \mu^+\mu^-)$ up to a few times 10^{-10}. In general, searches for BSM physics in charm FCNC processes are complementary to those in the B and K sector, since they provide unique access to up-type dynamics, the charm being the only up-type quark undergoing flavour oscillations.

In this Letter, the search for the $D^0 \to \mu^+\mu^-$ decay is performed using $D^{*+} \to D^0(\mu^+\mu^-)\pi^+$ decays, with the D^{*+} produced directly at a pp collision primary vertex (PV). The inclusion of charge conjugated processes is implied throughout the paper.

The data samples used in this analysis were collected during the year 2011 in pp collisions at a centre-of-mass energy of 7 TeV and correspond to an integrated luminosity of about 0.9 fb^{-1}.

2 Detector and simulation

The LHCb detector [7] is a single-arm forward spectrometer covering the pseudorapidity range $2 < \eta < 5$, designed for the study of particles containing b or c quarks. The detector includes a high precision tracking system consisting of a silicon-strip vertex detector surrounding the pp interaction region, a large-area silicon-strip detector located upstream of a dipole magnet with a bending power of about 4 Tm, and three stations of silicon-strip detectors and straw drift tubes placed downstream. The combined tracking system provides momentum measurement with relative uncertainty that varies from 0.4% at 5 GeV/c to 0.6% at 100 GeV/c, and an impact parameter (IP) resolution of 20 μm for tracks with high transverse momentum. Charged hadrons are identified using two

ring-imaging Cherenkov (RICH) detectors. Photon, electron and hadron candidates are identified by a calorimeter system consisting of scintillating-pad and pre-shower detectors, an electromagnetic calorimeter and a hadronic calorimeter. Muons are identified by a system composed of alternating layers of iron and multi-wire proportional chambers. The trigger consists of a hardware stage, based on information from the calorimeters and muon systems, followed by a software stage that applies a full event reconstruction [8].

Events are triggered and offline-selected in a way that is similar for the signal channel $D^{*+} \to D^0(\mu^+\mu^-)\pi^+$, the normalisation channel $D^{*+} \to D^0(\pi^+\pi^-)\pi^+$, and the control channels $J/\psi \to \mu^+\mu^-$, $D^{*+} \to D^0(K^-\pi^+)\pi^+$, and $D^0 \to K^-\pi^+$ selected without the D^* requirement.

All events are triggered at the hardware stage by requiring one muon with transverse momentum $p_T > 1.5$ GeV/c or two muons with $\sqrt{p_{T1} \times p_{T2}} > 1.3$ GeV/c. Decay channels with muons in the final state, $D^{*+} \to D^0(\mu^+\mu^-)\pi^+$ and $J/\psi \to \mu^+\mu^-$, are required to have one of the decay particles having triggered the event. Channels with only hadrons in the final state, $D^{*+} \to D^0(K^-\pi^+)\pi^+$, $D^{*+} \to D^0(\pi^+\pi^-)\pi^+$ and $D^0 \to K^-\pi^+$, are required to be triggered by particles other than those forming the candidate decay, called *spectator particles* in the following.

Exceptions to this trigger scheme are made for $J/\psi \to \mu^+\mu^-$ events, when used to determine the trigger efficiency, and $D^{*+} \to D^0(K^-\pi^+)\pi^+$ events, when used to determine the probability of hadron to muon misidentification, as described in Sections 4 and 5, respectively.

The software trigger selects events, for muonic final states, with either one track identified as a muon with $p_T > 1.0$ GeV/c and impact parameter with respect to the PV larger than 0.1 mm, or with two oppositely-charged tracks identified as muons, that form a vertex and have an invariant mass $m_{\mu^+\mu^-} > 1$ GeV/c^2. For hadronic final states, it selects events with at least one track with $p_T > 1.7$ GeV/c and $\chi^2_{IP} > 16$, where χ^2_{IP} is the difference between the χ^2 of the PV built with and without the considered track.

In a second stage, the software trigger uses algorithms that reconstruct two-body D^0 decays using exactly the same criteria as the offline selection for signal and control samples. In the software trigger, all selected final states are required to have one of the decay particles having triggered the event. Both $D^{*+} \to D^0(\pi^+\pi^-)\pi^+$ and $D^{*+} \to D^0(K^-\pi^+)\pi^+$ candidate events are prescaled to comply with the bandwidth requirements of the experiment.

Simulation samples are used for determining the relative efficiencies between the signal and the normalization modes: pp collisions are generated using PYTHIA 6.4 [9] with a specific LHCb configuration [10]; decays of hadronic particles are described by EVTGEN [11] in which final state radiation is generated using PHOTOS [12] and the interaction of the generated particles with the detector and its response are implemented using the GEANT4 toolkit [13] as described in Ref. [14].

3 Candidate selection

Candidate $D^0 \to \mu^+\mu^-$ decays are reconstructed in $D^{*+} \to D^0\pi^+$ decays. The two D^0 daughter tracks are required to be of good quality (χ^2 per degree of freedom (ndf) < 5) and to be displaced with respect to the closest PV, with χ^2_{IP} larger than 3 and 8 and p_{T} larger than 750 MeV/c and 1100 MeV/c. The D^0 secondary vertex (SV) is required to be of good quality ($\chi^2_{\mathrm{SV}} < 10$) and clearly separated from the PV in the forward direction (vertex separation $\chi^2 > 20$). When more than one PV per event is reconstructed, the one that gives the minimum χ^2_{IP} for the candidate is chosen. The D^0 candidate has to point to the PV ($\chi^2_{\mathrm{IP}} < 15$ and $\cos(\theta_{\mathrm{P}}) > 0.9997$, where θ_{P} is the angle between the D^0 momentum in the laboratory frame and the direction defined by the PV and SV) and have $p_{\mathrm{T}} > 1800$ MeV/c . The same selection is also applied to $J/\psi \to \mu^+\mu^-$ candidates, which are used for validating the muon identification and trigger efficiency derived from the simulation. Candidate D^0 (J/ψ) mesons are selected if their decay products have an invariant mass in the region of the known D^0 (J/ψ) mass.

An additional selection requirement, not applied at the trigger stage, is that the bachelor π^+ of the $D^{*+} \to D^0\pi^+$ decay has $\chi^2_{\mathrm{IP}} < 10$, $p_{\mathrm{T}} > 110$ MeV/c and is constrained to the PV using a Kalman filter (KF) [15]. This provides an improved resolution for the mass difference between the D^{*+} and D^0 candidates, $\Delta m_{h^+h^{(\prime)-}} \equiv m_{h^+h^{(\prime)-}\pi^+} - m_{h^+h^{(\prime)-}}$, where $h = \mu, \pi$ and $h' = K, \mu, \pi$. Candidates are selected with a mass difference value around 145.5 MeV/c^2.

After the selection, the background of the signal channel has two main sources: a peaking background due to two- and three-body D^0 decays, with one or two hadrons misidentified as muons, and combinatorial background due to semileptonic decays of beauty and charm hadrons. The former is reduced with tight particle identification criteria while the latter is reduced applying a multivariate selection.

The muon candidates in the D^0 decay are required to have associated muon chamber hits that are not shared with any other track in the event. A cut on a combined particle identification likelihood, aimed at separating muons from other particle species [16], is applied. This likelihood combines information about track-hit matching in the muon chambers, energy associated to the track in the calorimeters and particle identification in the RICH detectors. In order to explicitly veto kaons, thereby suppressing backgrounds such as $D^{*+} \to D^0(K^-\mu^+\nu_\mu)\pi^+$ decays, an additional cut on a particle identification likelihood aimed at separating kaons from other particle species [17] is applied. The remaining dominant source of pion to muon misidentification is due to pion decays in flight.

A boosted decision tree (BDT) [18], with the AdaBoost algorithm [19], provides a multivariate discriminant and is based on the following variables: χ^2_{KF} of the constrained fit, χ^2_{IP} of the D^0 vertex, D^0 pointing angle θ_{P}, minimum p_{T} and χ^2_{IP} of the two muons, positively-charged muon angle in the D^0 rest frame with respect to the D^0 flight direction and D^0 angle in the D^{*+} rest frame with respect to the D^{*+} flight direction. The BDT training makes use of $D^{*+} \to D^0(\mu^+\mu^-)\pi^+$ simulated events and $m_{\mu^+\mu^-}$ sideband data ($1810-1830$ MeV/c^2 and $1885-1930$ MeV/c^2); the data sample for the training consists of a separate sample of $80\,\mathrm{pb}^{-1}$, satisfying the same selection criteria, and is not used

in the search for the $D^0 \rightarrow \mu^+\mu^-$ decay. The absence of correlation between $m_{\mu^+\mu^-}$ and the BDT output variable is explicitly checked using data selected with the cuts $\Delta m_{\mu^+\mu^-} > 147$ MeV/c^2 and $m_{\mu^+\mu^-} > 1840$ MeV/c^2. The cut value on the BDT output variable is chosen in order to achieve the best expected limit on $\mathcal{B}(D^0 \rightarrow \mu^+\mu^-)$, based on simulated pseudo-experiments (see Section 6) assuming no signal, and has an efficiency of 74% on the signal while providing a reduction of more than a factor of three for the combinatorial background.

4   Normalisation

The $D^0 \rightarrow \mu^+\mu^-$ branching fraction is obtained from

$$\mathcal{B}(D^0 \rightarrow \mu^+\mu^-) = \frac{N_{\mu^+\mu^-}}{N_{\pi^+\pi^-}} \times \frac{\varepsilon_{\pi\pi}}{\varepsilon_{\mu\mu}} \times \mathcal{B}(D^0 \rightarrow \pi^+\pi^-) = \alpha \times N_{\mu^+\mu^-} \tag{1}$$

using the decay $D^{*+} \rightarrow D^0(\pi^+\pi^-)\pi^+$ as a normalisation mode, where α is the single event sensitivity, $N_{\pi^+\pi^-(\mu^+\mu^-)}$ are the yields and $\varepsilon_{\pi\pi(\mu\mu)}$ the total efficiencies for $D^{*+} \rightarrow D^0(\pi^+\pi^-)\pi^+$ ($D^{*+} \rightarrow D^0(\mu^+\mu^-)\pi^+$) decays. In this section the various contributions to α are determined.

The trigger efficiencies for the signal and normalisation channels are calculated using the simulation and corrected using data driven methods. To cross-check the signal trigger efficiency, $J/\psi \rightarrow \mu^+\mu^-$ events are selected in both data and simulation and triggered using spectator particles; consistency is observed within the relative statistical uncertainty of 2.7%. To cross-check the trigger efficiency for the normalisation channel, the trigger efficiency of the $D^0 \rightarrow K^-\pi^+$ decay is measured in a sub-sample of data taken with very loose trigger requirements. A correction factor for the trigger efficiency of $D^{*+} \rightarrow D^0(\pi^+\pi^-)\pi^+$ events as derived from the simulation is obtained, with a systematic uncertainty of 4.9%, mostly arising from the statistical uncertainty on the correction itself. The trigger efficiencies are found to be $(86.4\pm2.4)\%$ and $(3.3\pm0.2)\%$ for $D^{*+} \rightarrow D^0(\mu^+\mu^-)\pi^+$ and $D^{*+} \rightarrow D^0(\pi^+\pi^-)\pi^+$, respectively. The low efficiency of the hadronic channel comes from the requirement of the event being triggered by spectator particles.

The muon identification efficiency is also measured with simulated events and validated with a sample of $J/\psi \rightarrow \mu^+\mu^-$ decays triggered by spectator particles. The efficiency of the requirement of having associated hits in the muon chambers is determined using $J/\psi \rightarrow \mu^+\mu^-$ decays selected without muon identification requirements on one of the two tracks. The efficiency correction of the combined particle identification likelihood is determined comparing $J/\psi \rightarrow \mu^+\mu^-$ decays selected with the above muon identification criteria and in a kinematic of region of mean transverse momentum ($\langle p_{\mathrm{T}}(\mu) \rangle < 1\,\mathrm{GeV}/c$) and opening angle of the two muons in the plane transverse to the beam ($\Delta\phi < 1$ rad) which is similar to that of the $D^{*+} \rightarrow D^0(\mu^+\mu^-)\pi^+$ decays. Good agreement between data and simulation is observed within 2.6%, which is assigned as a systematic uncertainty.

Acceptance, reconstruction and selection efficiencies for the signal and normalisation channels are measured using simulated events. In order to estimate discrepancies between

data and simulation, the $D^{*+} \to D^0(K^-\pi^+)\pi^+$ channel, which benefits from high yield and low background, is used. Small deviations from the simulation shapes are observed in the D^0 daughter impact parameter, momentum and transverse momentum distributions. Since, for the branching fraction measurement, only the efficiency ratio matters, any systematic uncertainty related to these quantities cancels at first order. Indeed, varying the cuts, it is verified that the ratio of selection efficiencies changes by a negligible amount compared to other systematic uncertainties on α. The effect of interactions of the decay products with the detector material, different for muons and pions, results in an additional systematic uncertainty of 3% per track [20]. The selection and reconstruction efficiency ratio between the normalisation and signal channel is found to be 1.17±0.08, with the deviation from unity mostly coming from the muon identification efficiency.

The yield extraction for the normalisation channel is performed with an unbinned extended maximum likelihood fit to the two-dimensional distribution of $\Delta m_{\pi^+\pi^-}$ and $m_{\pi^+\pi^-}$. The probability density functions (PDFs) that parametrize the $\Delta m_{\pi^+\pi^-}$ distribution are a double Gaussian shape with common mean for the signal and the parametric function

$$f_\Delta(\Delta m_{\pi^+\pi^-}, a, b, c) = \left(1 - e^{-(\Delta m_{\pi^+\pi^-} - \Delta m_0)/c}\right) \times \left(\frac{\Delta m_{\pi^+\pi^-}}{\Delta m_0}\right)^a + b \times \left(\frac{\Delta m_{\pi^+\pi^-}}{\Delta m_0} - 1\right) \quad (2)$$

for the combinatorial background, where $\Delta m_0 = 139.6\,\mathrm{MeV}/c^2$ and a, b and c are fit parameters. For the $D^{*+} \to D^0(\pi^+\pi^-)\pi^+$ fit only the c parameter is varied and a and b are set to 0. The $m_{\pi^+\pi^-}$ distribution is parametrized with a Crystal Ball (CB) [21] function for the signal and a single exponential shape for the combinatorial background. The CB is a four-parameter function consisting of a Gaussian core, of mean μ and width σ, and a power-law low-end tail with negative slope n, below a threshold, defined by the ω parameter, at the value $\mu - \omega \times \sigma$. A small background component due to the random association of a $D^0 \to \pi^+\pi^-$ decay with a pion from the PV is also added to the fit, with the same PDF as the $D^{*+} \to D^0(\pi^+\pi^-)\pi^+$ for the $m_{\pi^+\pi^-}$ distribution, and the same f_Δ function as the combinatorial background for the $\Delta m_{\pi^+\pi^-}$ distribution. For the $D^{*+} \to D^0(K^-\pi^+)\pi^+$ component, a Gaussian PDF for the $\Delta m_{\pi^+\pi^-}$ distribution and a single exponential function for the $m_{\pi^+\pi^-}$ distribution are used.

Figure 1 shows the $\Delta m_{\pi^+\pi^-}$ and the $m_{\pi^+\pi^-}$ distributions for $D^{*+} \to D^0(\pi^+\pi^-)\pi^+$ from which a total yield of 6201±88 decays is estimated. The total uncertainty on the yield is dominated by statistics. It has been verified that alternative PDF parametrizations, such as modifications of the f_Δ function, do not lead to significant changes in the extracted $D^{*+} \to D^0(\pi^+\pi^-)\pi^+$ yields.

A single event sensitivity of $(3.00 \pm 0.27) \times 10^{-10}$ is obtained. The systematic contributions to α, together with the total uncertainty, obtained by summing in quadrature the individual contributions, are summarized in Table 1.
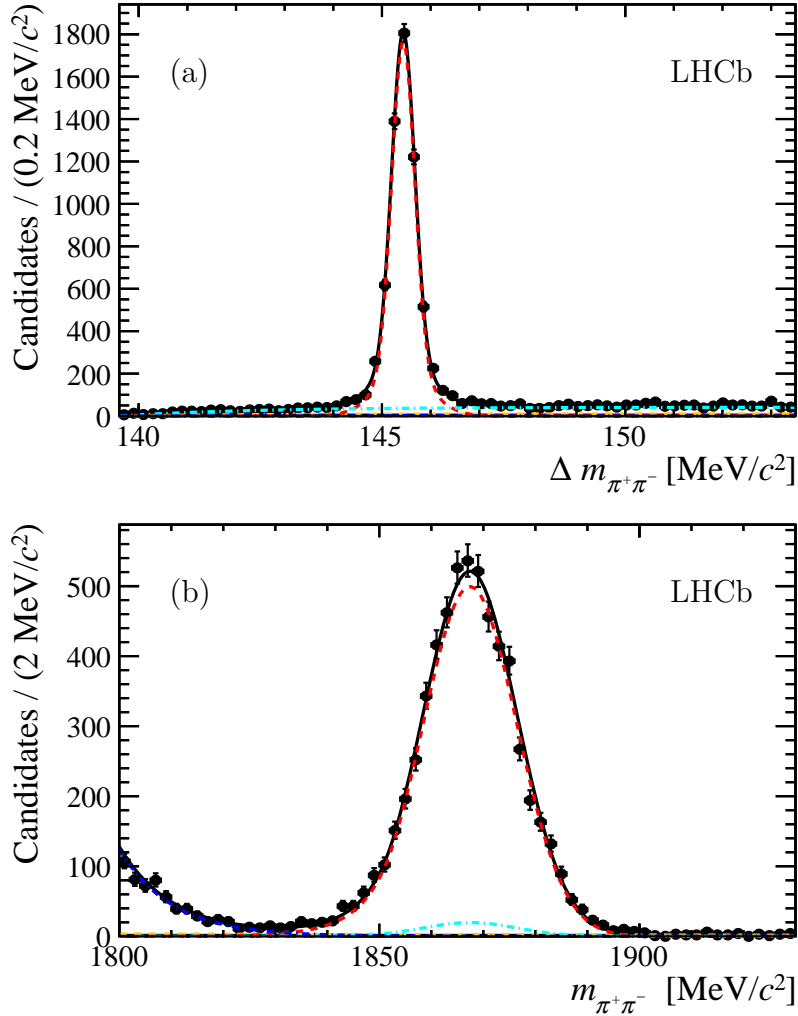
5

Figure 1: (a) Invariant mass difference $\Delta m_{\pi^+\pi^-}$, with $m_{\pi^+\pi^-}$ in the range $1840-1885$ MeV/c^2, and (b) invariant mass $m_{\pi^+\pi^-}$, with $\Delta m_{\pi^+\pi^-}$ in the range $144-147$ MeV/c^2, for $D^{*+} \to D^0(\pi^+\pi^-)\pi^+$ candidates in data. The projections of the two-dimensional unbinned extended maximum likelihood fit are overlaid. The curves represent the total (solid black), $D^{*+} \to D^0(\pi^+\pi^-)\pi^+$ (dashed red), the untagged $D^0 \to \pi^+\pi^-$ (dash-dotted cyan), the combinatorial background (dashed yellow) and the $D^{*+} \to D^0(K^-\pi^+)\pi^+$ (dash-dotted blue) contributions. The $D^{*+} \to D^0(\pi^+\pi^-)\pi^+$ candidates are prescaled at the software trigger stage by a factor 0.03.

5 Background yields from $D^{*+} \to D^0(\pi^+\pi^-)\pi^+$ decays

Due to the similar topology to the signal decay channel and the small difference between the pion and the muon mass, only the $D^{*+} \to D^0(\pi^+\pi^-)\pi^+$ decay can significantly con-

Table 1: Contributions to the systematic uncertainty of the single event sensitivity α.

Source	Relative uncertainty (%)
Material interactions	6.0
Muon identification efficiency	2.6
Hadronic trigger efficiency	4.9
Muon trigger efficiency	2.7
$\mathcal{B}(D^0 \to \pi^+\pi^-)$ [22]	1.9
Total systematic uncertainty	8.8

tribute as peaking background in both the $m_{\mu^+\mu^-}$ and $\Delta m_{\mu^+\mu^-}$ distributions when the two pions are misidentified as muons.

The yield of misidentified $D^{*+} \to D^0(\pi^+\pi^-)\pi^+$ decays, $N_{\pi^+\pi^- \to \mu^+\mu^-}$, is obtained from the yield of selected $D^{*+} \to D^0(\pi^+\pi^-)\pi^+$ events, $N_{\pi^+\pi^-}$, as

$$N_{\pi^+\pi^- \to \mu^+\mu^-} = N_{\pi^+\pi^-} \times \frac{\varepsilon_{\pi\pi \to \mu\mu}}{\varepsilon_{\pi\pi}} \tag{3}$$

where $\varepsilon_{\pi\pi \to \mu\mu}$ is the total efficiency for $D^{*+} \to D^0(\pi^+\pi^-)\pi^+$ events with both pions misidentified as muons. Both the efficiencies in the numerator and denominator are obtained from the simulation of a very large $D^{*+} \to D^0(\pi^+\pi^-)\pi^+$ event sample and corrections are applied using data driven methods. The main systematic uncertainties in Eq. 3 come from the trigger efficiency for $D^{*+} \to D^0(\pi^+\pi^-)\pi^+$ events, as discussed in Section 4, and the misidentification probability, which is cross-checked with data using $D^{*+} \to D^0(K^-\pi^+)\pi^+$ events.

The invariant mass difference $\Delta m_{K^-\pi^+}$ and invariant mass $m_{K^-\pi^+}$ distributions in data for $D^{*+} \to D^0(K^-\pi^+)\pi^+$ candidates, with muon identification applied to the pion and triggered by spectator particles with respect to the D^0 daughter pion, are shown in Fig. 2. These distributions show some remarkable differences compared to those of Fig. 1: a tail appears on the left of the peak in the $m_{K^-\pi^+}$ distribution and the $\Delta m_{K^-\pi^+}$ and $m_{K^-\pi^+}$ distributions display a broader mass distribution. As the simulation shows, the left-hand tail in the $m_{K^-\pi^+}$ distribution comes from two effects of comparable size, a low mass tail of the $D^{*+} \to D^0(K^-\pi^+)\pi^+$ decays due to the momentum loss in the pion decay and a high mass tail of $D^{*+} \to D^0(K^-\mu^+\nu_\mu)\pi^+$ decays, the latter also contributing to the broadening of the mass resolution of the $\Delta m_{K^-\pi^+}$ distribution. To suppress the background from $D^{*+} \to D^0(K^-\mu^+\nu_\mu)\pi^+$ decays, the measurement of the misidentification probability is performed using only the candidates on the upper side of the $m_{K^-\pi^+}$ peak, taking the ratio of events with and without the muon identification applied to the pion. A correction factor of 1.2 ± 0.1, taking into account the event yield in the pion decay tail, is applied.

The single pion to muon misidentification probability in data is $(2.9 \pm 0.2) \times 10^{-3}$, with a ratio of data to simulation of 0.88 ± 0.15. This latter value, squared, is used as
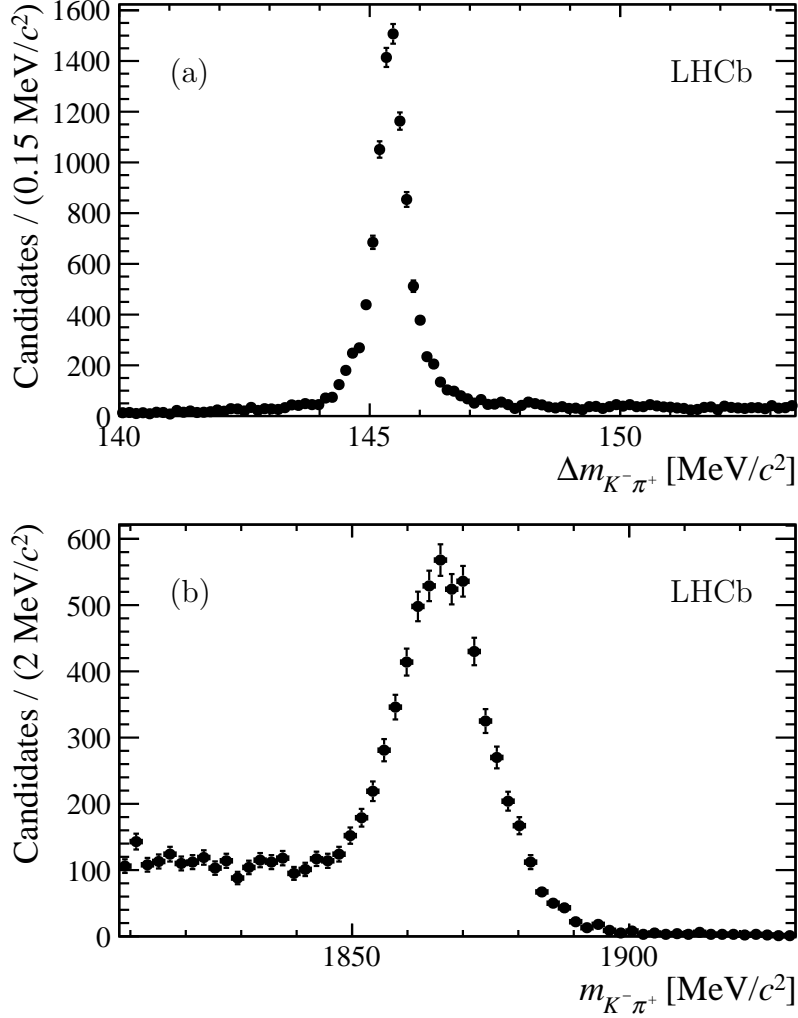
Figure 2: (a) Invariant mass difference $\Delta m_{K^-\pi^+}$ and (b) invariant mass $m_{K^-\pi^+}$ distributions in data for $D^{*+} \to D^0(K^-\pi^+)\pi^+$ candidates, with muon identification applied to the pion. The events are triggered by spectator particles with respect to the D^0 daughter pion. The $D^{*+} \to D^0(K^-\pi^+)\pi^+$ candidates are prescaled at the software trigger stage by a factor 0.15.

a correction factor for $\varepsilon_{\pi\pi\to\mu\mu}$ as determined from the simulation. A reweighting of the single misidentification probability taking into account the momentum correlation of the two D^0 daughter pions gives consistent results within the uncertainties. It is also verified that the small difference in the momentum distribution between data and simulation has a negligible impact on the determination of the misidentification probability.

The number of expected doubly-misidentified $D^{*+} \to D^0(\pi^+\pi^-)\pi^+$ decays in our data sample is 45 ± 19.

The determination of the number of doubly-misidentified events is cross-checked by considering the observed number of $D^{*+} \to D^0(K^-\pi^+)\pi^+$ candidates with double misiden-
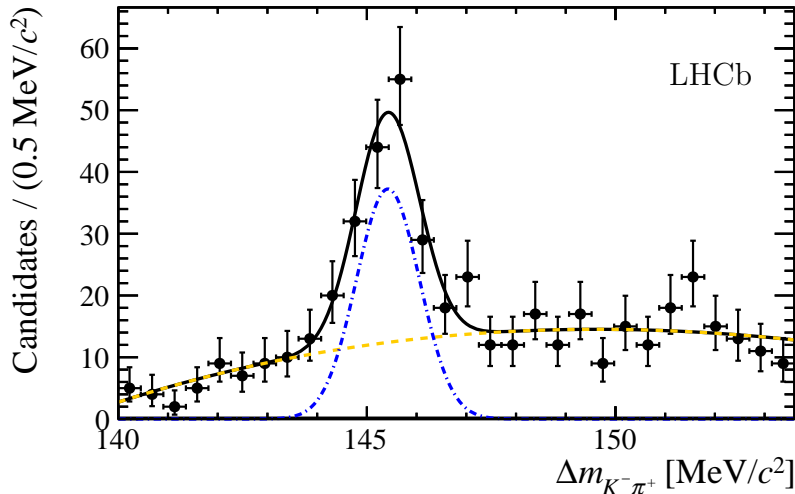
Figure 3: Invariant mass difference $\Delta m_{K^-\pi^+}$ for $D^{*+} \to D^0(K^-\pi^+)\pi^+$ candidates, with both hadrons misidentified as muons, with $m_{\mu^+\mu^-}$ in the range $1720-1800$ MeV/c^2. The two muons are reconstructed using the $K\pi$ and πK mass hypotheses. The result of the unbinned extended maximum likelihood fit is overlaid. The curves represent the total distribution (solid black), the combinatorial background (dashed yellow) and the $D^{*+} \to D^0(K^-\pi^+)\pi^+$ (dash-dotted blue) contribution.

tification in the lower sideband of the $m_{\mu^+\mu^-}$ distribution, extending in the selection down to 1720 MeV/c^2. The yield of these events is determined from an unbinned extended maximum likelihood fit to the $\Delta m_{K^-\pi^+}$ distribution, where the two muons are reconstructed using the $K\pi$ and πK mass hypotheses, requiring $m_{\mu^+\mu^-} < 1800$ MeV/c^2, as shown in Fig. 3. The PDFs used for the fit are a single Gaussian shape for the $D^{*+} \to D^0(K^-\pi^+)\pi^+$ events with floating mean and width and an f_Δ function for the background, will all three a, b and c parameters allowed to vary. To obtain a prediction for the number of misidentified $D^{*+} \to D^0(\pi^+\pi^-)\pi^+$ decays, the number of $D^{*+} \to D^0(K^-\pi^+)\pi^+$ candidates is multiplied by the ratio of $D^0 \to \pi^+\pi^-$ to $D^0 \to K^-\pi^+$ branching fractions and by the ratio of pion to muon and kaon to muon misidentification probabilities, assuming factorization of the misidentification probabilities of the two D^0 daughters. The kaon to muon misidentification probability is measured with $D^{*+} \to D^0(K^-\pi^+)\pi^+$ decays, triggered by spectator particles with respect to the kaon, and is found to be $(6.3\pm0.6)\times10^{-4}$. This very small value is achieved using the kaon veto based on the RICH detectors, as described in Section 3. The estimated yield of $D^{*+} \to D^0(\pi^+\pi^-)\pi^+$ is compatible with that obtained from the method described above, though with a larger uncertainty.

6 Results

The search for the $D^0 \to \mu^+\mu^-$ decay is performed using an unbinned extended maximum likelihood fit to the two-dimensional distribution of $\Delta m_{\mu^+\mu^-}$ and $m_{\mu^+\mu^-}$. The five different fit components are the signal $D^{*+} \to D^0(\mu^+\mu^-)\pi^+$, the combinatorial background and the background from $D^{*+} \to D^0(\pi^+\pi^-)\pi^+$, $D^{*+} \to D^0(K^-\pi^+)\pi^+$ and $D^{*+} \to D^0(\pi^-\mu^+\nu_\mu)\pi^+$ decays.

The PDF shapes are chosen as detailed in Table 2. The parameter input values are determined from the simulation of the individual channels, except for the combinatorial background, which is assumed to have a smooth distribution across the whole invariant mass difference $\Delta m_{\mu^+\mu^-}$ and invariant mass $m_{\mu^+\mu^-}$ ranges, as in the $D^{*+} \to D^0(\pi^+\pi^-)\pi^+$ fit of Section 4. The table also shows the corresponding fit parameters that are allowed to vary, both freely and with Gaussian constraints. Other fit parameters, not included in the table, are fixed to the values obtained from the simulation. It is explicitly checked that the final result is insensitive to the variation of these parameters.

The width of the CB function describing the $D^{*+} \to D^0(\pi^+\pi^-)\pi^+$ background in the $m_{\mu^+\mu^-}$ distribution and the narrower width of the double Gaussian shape describing the $D^{*+} \to D^0(\pi^+\pi^-)\pi^+$ background in the $\Delta m_{\mu^+\mu^-}$ distribution are corrected for the broader mass distribution observed in data; the widths are increased by about 40% in $\Delta m_{\mu^+\mu^-}$ and 25% in $m_{\mu^+\mu^-}$. The CB slope parameter is fixed to the mean value obtained from simulation. Varying this value within its uncertainty leads to a negligible change in the final result.

The $D^{*+} \to D^0(K^-\pi^+)\pi^+$ and $D^{*+} \to D^0(\pi^-\mu^+\nu_\mu)\pi^+$ yields are normalized to the $D^{*+} \to D^0(\pi^+\pi^-)\pi^+$ yields based on their relative branching fractions, on the number of generated events and on the pion to muon and kaon to muon misidentification probabilities, as measured from data. To take into account discrepancies between data and simulation for these two latter quantities, a conservative uncertainty of 50% and 30% is assigned, respectively.

The signal PDFs are parametrised as in the $D^{*+} \to D^0(\pi^+\pi^-)\pi^+$ fit of Section 4 and the shape parameters are fixed to the $D^{*+} \to D^0(\pi^+\pi^-)\pi^+$ output fit values. A variation of these parameters within their uncertainties give a negligible effect on the final value for $\mathcal{B}(D^0 \to \mu^+\mu^-)$.

The systematic uncertainties related to both the normalisation, through α, and the background shapes and yields, are included in the fit as Gaussian constraints to the parameters.

After the fit, all constrained parameters converged to the input values within a few percent but $\varepsilon_{\pi\pi\to\mu\mu}$ and ω, which changed by about $+16\%$ and -20%, respectively, though remaining consistent with the fit input values, within the uncertainty.

Figure 4 shows the $\Delta m_{\mu^+\mu^-}$ and $m_{\mu^+\mu^-}$ distributions, together with the one-dimensional binned projections of the two-dimensional fit overlaid. The χ^2/ndf of the fit projections are 1.0 and 1.3, corresponding to probabilities of 44% and 19%, respectively. The data are consistent with the expected backgrounds. In particular, a residual contribution from $D^{*+} \to D^0(\pi^+\pi^-)\pi^+$ events is visible among the peaking backgrounds.

Table 2: PDF components describing $m_{\mu^+\mu^-}$ and $\Delta m_{\mu^+\mu^-}$ distributions in the signal and corresponding freely varying and Gaussian constrained fit parameters. The coefficients of the exponential (EXP) function used to describe both the $D^{*+} \to D^0(K^-\pi^+)\pi^+$ and $D^{*+} \to D^0(\pi^-\mu^+\nu_\mu)\pi^+$ backgrounds are $\gamma_{K\pi}$ and $\gamma_{\pi\mu\nu}$ while $f_{K\pi}$ and $f_{\pi\mu\nu}$ are the normalisation factors to the $D^{*+} \to D^0(\pi^+\pi^-)\pi^+$ events. The symbols $\langle \Delta m_{\mu^+\mu^-} \rangle_\eta$, $\eta = i, j$ and k represent the mean values and $(\sigma_1^\Delta)_\eta$ the narrower width of the double Gaussian (DG) PDF describing $D^{*+} \to D^0(\pi^+\pi^-)\pi^+$, $D^{*+} \to D^0(K^-\pi^+)\pi^+$ and $D^{*+} \to D^0(K^-\mu^+\nu_\mu)\pi^+$ distributions (for $D^{*+} \to D^0(K^-\pi^+)\pi^+$ a single Gaussian (SG) PDF is used). The normalisation for the $D^{*+} \to D^0(\pi^+\pi^-)\pi^+$ event yield is obtained from the procedure described in Section 5. The function f_m is a constant. The parameters ω, μ and σ of the Crystal Ball function describing the $D^{*+} \to D^0(\pi^+\pi^-)\pi^+$ events are described in Section 4.

Fit component	$m_{\mu^+\mu^-}$	$\Delta m_{\mu^+\mu^-}$	Free	Constrained
Combinatorial	f_m	f_Δ	yield, a, b, c	
$D^{*+} \to D^0(\pi^+\pi^-)\pi^+$	CB	DG		α, $\varepsilon_{\pi\pi\to\mu\mu}$, ω, μ, σ, $\langle\Delta m_{\mu^+\mu^-}\rangle_i$, $(\sigma_1^\Delta)_i$
$D^{*+} \to D^0(K^-\pi^+)\pi^+$	EXP	SG		$\gamma_{K\pi}$, $f_{K\pi}$, $\langle\Delta m_{\mu^+\mu^-}\rangle_j$, $(\sigma^\Delta)_j$
$D^{*+} \to D^0(\pi^-\mu^+\nu_\mu)\pi^+$	EXP	DG		$\gamma_{\pi\mu\nu}$, $f_{\pi\mu\nu}$, $\langle\Delta m_{\mu^+\mu^-}\rangle_k$, $(\sigma_1^\Delta)_k$
$D^{*+} \to D^0(\mu^+\mu^-)\pi^+$	CB	DG	yield	

The value obtained for the $D^0 \to \mu^+\mu^-$ branching fraction is $(0.09 \pm 0.30) \times 10^{-8}$. Since no significant excess of signal is observed with respect to the expected backgrounds, an upper limit is derived. The limit determination is performed, in the RooStats framework [23], using the asymptotic CL_s method [24]. This is an approximate method, equivalent to the true CL_s method performed with simulated pseudo-experiments, when the data samples are not too small.

Figure 5 shows the expected and observed CL_s as a function of the assumed $D^0 \to \mu^+\mu^-$ branching fraction. The expected upper limit is $5.5\ (6.7)^{+3.1}_{-2.0} \times 10^{-9}$ at 90% (95%) CL, while the observed limit is $6.2\ (7.6) \times 10^{-9}$ at 90% (95%) CL. The p-value for the background-only hypothesis is 0.4.

The robustness of the fit procedure is tested with simulated pseudo-experiments using the same starting values for the fit parameters used in the data fit except for the combinatorial background PDF, for which the fitted parameters from data are used. Simulated pseudo-experiments are performed corresponding to $D^0 \to \mu^+\mu^-$ branching fraction values of 0, 10^{-8} and 5×10^{-8}. In all cases the results reproduce the input values within the estimated uncertainties.

Several systematic checks are performed varying the selection requirements, including the muon identification criteria, varying the parametrization of the fit components and the fit range and removing the multivariate selection. The measured $\mathcal{B}(D^0 \to \mu^+\mu^-)$ does not change significantly with these variations.

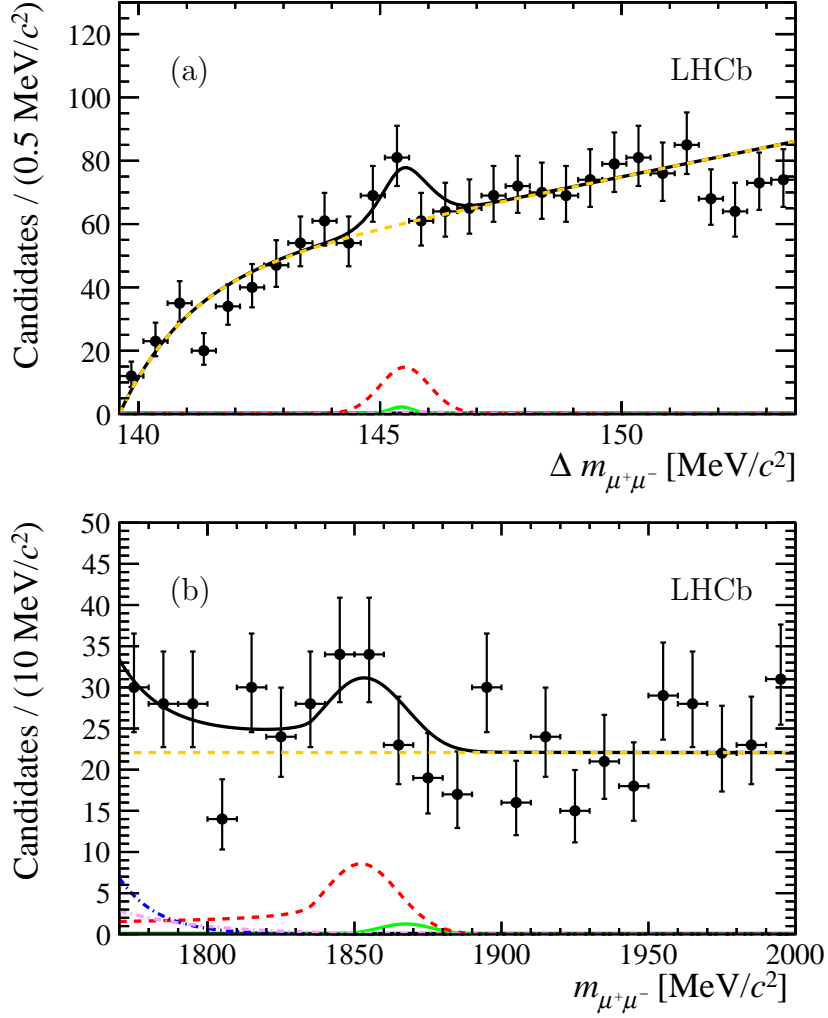Figure 4: (a) Invariant mass difference $\Delta m_{\mu^+\mu^-}$, with $m_{\mu^+\mu^-}$ in the range $1820-1885$ MeV/c^2 and (b) invariant mass $m_{\mu^+\mu^-}$, with $\Delta m_{\mu^+\mu^-}$ in the range $144-147$ MeV/c^2 for $D^{*+} \to D^0(\mu^+\mu^-)\pi^+$ candidates. The projections of the two-dimensional unbinned extended maximum likelihood fit are overlaid. The curves represent the total distribution (solid black), the $D^{*+} \to D^0(\pi^+\pi^-)\pi^+$ (dashed red), the combinatorial background (dashed yellow), the $D^{*+} \to D^0(K^-\pi^+)\pi^+$ (dash-dotted blue), the $D^{*+} \to D^0(\pi^-\mu^+\nu_\mu)\pi^+$ (dash-dotted purple) and the signal $D^{*+} \to D^0(\mu^+\mu^-)\pi^+$ (solid green) contribution.

To test the dependence of the result on the knowledge of the double misidentification probability, the uncertainty is doubled in the fit input; $\mathcal{B}(D^0 \to \mu^+\mu^-)$ is consistent with the baseline result.

In addition, the robustness of the result is checked by artificially increasing the value of the kaon to muon misidentification as determined from data in Section 5 up to 200% of its measured value, and the fitted branching fraction still remains consistent with no
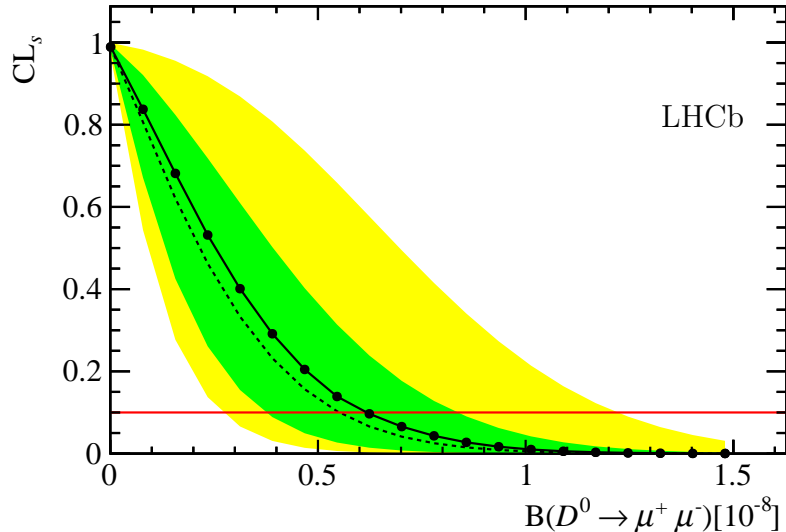
Figure 5: CL_s (solid line) as a function of the assumed $D^0 \to \mu^+\mu^-$ branching fraction and median (dashed line), 1σ and 2σ bands of the expected CL_s, in the background-only hypothesis, obtained with the asymptotic CL_s method. The horizontal line corresponding to CL_s=0.05 is also drawn.

significant excess of signal with respect to the background expectations.

7 Summary

A search for the rare decay $D^0 \to \mu^+\mu^-$ is performed using a data sample, corresponding to an integrated luminosity of 0.9 fb^{-1}, of pp collisions collected at a centre-of-mass energy of 7 TeV by the LHCb experiment. The observed number of events is consistent with the background expectations and corresponds to an upper limit of

$$\mathcal{B}(D^0 \to \mu^+\mu^-) < 6.2\,(7.6) \times 10^{-9} \text{ at } 90\%\,(95\%) \text{ CL.}$$

This result represents an improvement of more than a factor twenty with respect to previous measurements but remains several orders of magnitude larger than the SM prediction.

Acknowledgements

References

[1] S. Glashow, J. Iliopoulos, and L. Maiani, *Weak interactions with lepton-hadron symmetry*, Phys. Rev. **D2** (1970) 1285.

[2] G. Burdman, E. Golowich, J. L. Hewett, and S. Pakvasa, *Rare charm decays in the standard model and beyond*, Phys. Rev. **D66** (2002) 014009, `arXiv:hep-ph/0112235`.

[3] BaBar collaboration, J. P. Lees *et al.*, *Search for the decay $D^0 \to \gamma\gamma$ and measurement of the branching fraction for $D^0 \to \pi^0\pi^0$*, Phys. Rev. **D85** (2012) 091107, `arXiv:1110.6480`.

[4] Belle collaboration, M. Petric *et al.*, *Search for leptonic decays of D^0 mesons*, Phys. Rev. **D81** (2010) 091102, `arXiv:1003.2345`.

[5] G. Burdman and I. Shipsey, *D^0 - $\bar{D}^0$ mixing and rare charm decays*, Ann. Rev. Nucl. Part. Sci. **53** (2003) 431, `arXiv:hep-ph/0310076`.

[6] A. Paul, A. de La Puente, and I. I. Bigi, *Manifestations of warped extra dimension in rare charm decays and asymmetries*, `arXiv:1212.4849`.

[7] LHCb collaboration, A. A. Alves Jr. *et al.*, *The LHCb detector at the LHC*, JINST **3** (2008) S08005.

[8] R. Aaij *et al.*, *The LHCb trigger and its performance in 2011*, JINST **8** (2013) P04022, `arXiv:1211.3055`.

[9] T. Sjöstrand, S. Mrenna, and P. Z. Skands, *PYTHIA 6.4 physics and manual*, JHEP **05** (2006) 026, `arXiv:hep-ph/0603175`.

[10] I. Belyaev *et al.*, *Handling of the generation of primary events in* GAUSS, *the LHCb simulation framework*, Nuclear Science Symposium Conference Record (NSS/MIC) **IEEE** (2010) 1155.

[11] D. J. Lange, *The EvtGen particle decay simulation package*, Nucl. Instrum. Meth. **A462** (2001) 152.

[12] P. Golonka and Z. Was, *PHOTOS Monte Carlo: a precision tool for QED corrections in Z and W decays*, Eur. Phys. J. **C45** (2006) 97, arXiv:hep-ph/0506026.

[13] GEANT4 collaboration, J. Allison *et al.*, *Geant4 developments and applications*, IEEE Trans. Nucl. Sci. **53** (2006) 270; GEANT4 collaboration, S. Agostinelli *et al.*, *GEANT4: A simulation toolkit*, Nucl. Instrum. Meth. **A506** (2003) 250.

[14] M. Clemencic *et al.*, *The LHCb simulation application, GAUSS: design, evolution and experience*, J. Phys. : Conf. Ser. **331** (2011) 032023.

[15] W. D. Hulsbergen, *Decay chain fitting with a Kalman filter*, Nucl. Instrum. Meth. **A552** (2005) 566, arXiv:physics/0503191.

[16] A. A. Alves *et al.*, *Performance of the LHCb muon system*, JINST **8** (2013) P02022, arXiv:1211.1346.

[17] M. Adinolfi *et al.*, *Performance of the LHCb RICH detector at the LHC*, arXiv:1211.6759, to appear in Eur. Phys. J. C.

[18] L. Breiman, J. H. Friedman, R. A. Olshen, and C. J. Stone, *Classification and regression trees*. Wadsworth international group, Belmont, California, USA, 1984.

[19] R. E. Schapire and Y. Freund, *A decision-theoretic generalization of on-line learning and an application to boosting*, Jour. Comp. and Syst. Sc. **55** (1997) 119.

[20] LHCb collaboration, R. Aaij *et al.*, *Measurement of $\sigma(pp \to b\bar{b}X)$ at $\sqrt{s} = 7$ TeV in the forward region*, Phys. Lett. **B694** (2010) 209, arXiv:1009.2731.

[21] T. Skwarnicki, *A study of the radiative cascade transitions between the Upsilon-prime and Upsilon resonances*. PhD thesis, Institute of Nuclear Physics, Krakow, 1986.

[22] Particle Data Group, J. Beringer *et al.*, *Review of particle physics*, Phys. Rev. D **86** (2012) 010001.

[23] L. Moneta *et al.*, *The RooStats project*, PoS **ACAT2010** (2010) 057, arXiv:1009.1003.

[24] G. Cowan, K. Cranmer, E. Gross, and O. Vitells, *Asymptotic formulae for likelihood-based tests of new physics*, Eur. Phys. J. C **71** (2011) 1554, arXiv:1007.1727.